COSMIC STRUCTURE FORMATION AND THE BACKGROUND RADIATION

J. Richard Bond

CIAR Cosmology Program
Canadian Institute for Theoretical Astrophysics
McLennan Physics Labs, University of Toronto
Toronto ON M5S 1A7, Canada

ABSTRACT

I describe our post-COBE theories for how structure developed in the Universe, from the ultra-large scales beyond that little bit of the Universe accessible to our observations to 'short-distance' scales where gas dynamical processes will have been as important as gravity in shaping the high redshift objects that formed. In between lie the very large scales whose gravitational potential fluctuations are what we believe the COBE DMR experiment has detected; large scales probed by galaxy and cluster clustering, by the streaming motions of galaxies, and, most importantly, by intermediate angle microwave background experiments. Together with COBE, we have hopes that these probes can pin down the parameters of the cosmological model, including the amplitude and shape of the primordial spectrum of gravitational metric fluctuations from whose instability the structure around us springs. An initially scale invariant spectrum or something close to it connects through a hundred-fold extrapolation in wavelength the COBE detection to observations of galaxy clustering. Although this is a spectacular confirmation of the general thrust of the inflation-based theoretical work of the past decade, and is consistent with the 'standard' cold dark matter model, albeit with more nonlinear dynamics than most theorists are comfortable with, reconciliation of the observed large scale power in the galaxy distribution with the COBE amplitude may require variations on the basic theme, involving such exotica as a nonzero cosmological constant, a whiff of hot dark matter (*i.e.*, few eV neutrinos), extended, natural or power law inflation, non-local biasing of the galaxy distribution relative to the dark matter distribution, gravity wave induced temperature anisotropies, *etc.*

© J. R. Bond 1993

1. Introduction

In this review, I shall assume the reader is reasonably familiar with cosmological ideas. An Appendix is added to introduce a number of the relevant concepts. In §2, I describe current uncertainties in the 'global parameters' of the Universe that define the cosmological model, since it is within those bounds that a theory of cosmic structure must reside. In §3, I briefly review the major ideas for the origins of the fluctuations that grew through gravitational instability to the current structure we observe. Inflation-induced perturbations have been the leading contender for a decade and this has been reinforced by COBE's detection. §4 gives the main message of this paper: how probes covering all of the spatial wavebands from the very large to the very small are combining to tell us the story of how cosmic structure arose. And the techniques are as diverse as: microwave anisotropy experiments on satellites, balloons and at the South Pole; redshift surveys and deep angular surveys of galaxies and clusters; streaming motion probes using 21 cm observations of galaxies; X-ray and microwave background observations of the hot gas in clusters; optical and sub-mm observations of high redshift objects, quasars, starbursters, radio galaxies, faint blue galaxies, dwarf galaxies, intergalactic (Lyman alpha) gas clouds, 'normal' galaxies, *etc.*

§5 introduces a few representative 'post-COBE' theories of structure formation. It also casts the statistical significance of the COBE detection in terms of a likelihood function. Other experiments are beginning to see microwave anisotropies as well, and the beginnings of that tale are given in §5 with likelihood functions for two other experiments that probe somewhat smaller angular scales than COBE does. An MIT balloon experiment confirms what COBE has seen and a South Pole experiment has seen what could turn out to be a cosmic signal. *All* anisotropy experiments are now reporting detections of something, but separating the cosmic from the merely Galactic is a challenge for our community. §6 shows how the large scale clustering data is moving us away from the simplest version of the inflation-inspired cold dark matter model which has dominated theoretical thinking for the past decade. The crucial role that clusters play in fixing the structure formation model is then described. In §7, I sketch some of the complications that arise at smaller scales as a result of 'gastrophysical' processes, for the development of galaxies and the intergalactic medium, as cooling, radiant energy from stars and black hole accretion, and supernova winds separate the gas from the collisionless dark matter. Even so, observations of cosmic objects when the Universe was a factor of 2 to 10 smaller will offer invaluable if somewhat dirty probes of the short distance behaviour of the structure formation theory.

Given the gravitational instability of the Universe and the high degree of isotropy of the cosmic background radiation, viewing the development of cosmic structure through the evolution and coupling of perturbation eigenmodes is a very instructive approach. On scales much smaller than any global curvature scale, these eigenmodes are simply plane waves characterized by spatial wavenumbers k (with the average time-dependent expansion factor $a(t)$ of the Universe factored out). We may roughly divide the problem of cosmic structure formation into various wavebands, which we discuss in turn in the following sections. (We normalize a to be unity now so that comoving wavelengths, $2\pi k^{-1}$, are expressed in current cosmic length units. Since these are estimated from recession velocities, the unit is the $\mathrm{h^{-1}Mpc}$, where h is the Hubble parameter in units of 100 km $\mathrm{s^{-1}\,Mpc^{-1}}$. $a^{-1}-1$ is the redshift at time t.

• *ULSS*: The realm of ultra-large-scale-structure corresponds to spatial comoving (inverse) wavenumbers k^{-1} in excess of a few times the Hubble radius, $cH_0^{-1} = 3000\,\mathrm{h^{-1}Mpc}$. Of course, we only access our 'Hubble patch,' which we think is more likely to be just a tiny bit of the Universe rather than the bulk of it, although we cannot know what lies beyond nor how geometrically complex it is. Mean properties of our bit such as curvature are what we usually misname 'global parameters.'

• *VLSS*: Over the realm of very-large-scale-structure, from the horizon scale ($k^{-1} \sim 2cH_0^{-1}$ for Einstein-deSitter models) down to say $k^{-1} \sim 100\,\mathrm{h^{-1}Mpc}$, density and velocity fluctuations are so small that no influence on observed cosmic structures will be likely, but gravitational potential perturbations are large enough to be observed through their influence on the cosmic background radiation (CMB) – COBE and other large angle experiments probe VLSS directly. In most models, the fluctuation spectrum shape is unmodified over its initial shape (the transfer function is approximately unity), which further simplifies the interpretation of the VLSS CMB probes (§4).

• *LSS*: Over the realm of large scale structure, from $\sim 100\,\mathrm{h^{-1}Mpc}$ down to about $5\,\mathrm{h^{-1}Mpc}$, the transfer function does change, and depends upon the type and density of dark matter, on the values of Λ, Ω, H_0, *etc.* However, we believe that the evolution of the waves in this band is sufficiently linear that first order perturbation calculations of LSS probes may be valid. Intermediate angle CMB anisotropy experiments in conjunction with the VLSS probes will be particularly invaluable for pinning down cosmological parameters. Building a consistent picture with LSS flow and clustering data will be a major area over the next few years.

• *MSS, SSS, VSSS, USSS*: Below LSS lie wavebands for which gas physics will have been extremely important, if not dominant, in determining the nature of the objects we see and how they are clustered. Fluctuations are nonlinear in these regimes. In a hierarchical model, nonlinearity at different scales will occur at sufficiently different epochs that we divide the gastrophysical realms into medium, small, very small and ultra small, bands responsible for the construction of, respectively: clusters and groups ($\sim 10^{14-15}\,\mathrm{M_\odot}$); bright galaxies ($\sim 10^{11-12}\,\mathrm{M_\odot}$); dwarf galaxies and Lyman alpha clouds ($\sim 10^{9-10}\,\mathrm{M_\odot}$); and the first gas clouds to collapse ($\sim 10^{6-7}\,\mathrm{M_\odot}$), which make the first stars. Of

course, significant gas dynamical processing may obscure the hierarchical relationship between object and primordial fluctuation waveband.

2. The Ultra-Large Scale Parameters of our Hubble Patch

All that we know of ultra-large structure are single values, averages over our local Hubble patch that probably tell us little about the entire global structure of the Universe, in spite of the folklore that Ω for our patch defines the global fate. Thus even if we measure an average density $\bar{\rho} < \rho_{crit}$ now, our ancestors, if they exist in such a distant future, may learn that $\bar{\rho} > \rho_{crit}$ over far larger scales than H_0^{-1}. Our current Hubble patch would then be a local void expanding into denser ridges, and the whole may eventually collapse; and beyond this, an ultra-ultra-large patch within which our island of reheated stuff resides will still be accelerating (*i.e.*, inflating) — according to the theory of stochastic inflation. The evolution of the substructure in our Hubble patch and the propagation of photons in it very much depends upon these mean parameters.

T_γ: The relic photon temperature is now well determined, from COBE's FIRAS and Gush, Halpern and Wishnow's COBRA experiments. The FIRAS team has recently announced $T_\gamma = 2.726 \pm 0.005$ (1 sigma error, Mather *et al.* [1]).

N_ν: The number of light relic neutrinos is 3, determined within a few percent, using the CERN LEP and SLAC SLC data on Z_0 boson decay. With T_γ and a little weak interaction theory, we get T_ν, and thus the number density of light relic neutrinos; the direct detection of this sea seems very unlikely.

Ω_B: The baryon abundance parameter appears to be well constrained by Big Bang nucleosynthesis, especially with advances in neutron lifetime measurements and determination of the light neutrino number. The upper bound, based primarily upon the requirement that He^4 is not overproduced, is $\Omega_B \lesssim 0.064\,(2h)^{-2}$ (*e.g.,* Olive *et al.* [2]). If the combination of He^3+D is not mostly destroyed during stellar evolution, there is also a lower bound, $\Omega_B \gtrsim 0.038\,(2h)^{-2}$. Steigman and collaborators [2] use Lithium observations to argue that the error on $\Omega_B \approx 0.06\,(2h)^{-2}$ is under 10%! If nucleosynthesis was inhomogeneous, Ω_B could be as high as 0.3; however, the quark-hadron phase transition would have to have been first order in this theory, and recent lattice gauge theory simulations suggest it wasn't (with the caveat that this relies upon an ability to scale from very small computational lattices to predict the continuum result).

Remnant Dark Matter: The allowed range for Ω_B should be compared with the ~ 0.007 observed in luminous baryons, suggesting at least some baryonic dark matter exists. The form it takes, whether in Jupiters and brown dwarfs, in very massive black holes, or in warm gas, is a decidedly gastrophysical problem.

Relic Dark Matter: Dynamical estimates of the amount of dark matter from combining the observed mass-to-light ratios in galaxies and clusters with the observed luminosity density typically give ~ 0.1–0.3 of the closure density. Comparison of IRAS galaxy redshift surveys with surveys in which radial distance is also estimated gives a value nearer unity. Biasing of the galaxy distribution relative to the dark matter distribution would raise these estimates. Thus, there is no evidence against Ω in clustering dark matter being nearly unity. The most popular candidate for the clustering dark matter is cold dark matter — massive slowly moving elementary particle relics of the early universe. Most people's best bet for CDM remains the lightest supersymmetric particle, even though the LEP results from CERN on the Z_0-boson lifetime give surprisingly strong constraints on the properties of generic massive CDM candidates with interactions that are weak or weaker than weak. The axion remains as viable as ever.

In the past few years hot dark matter in the form of a light neutrino (in the ev range and presumably a ν_τ) got a powerful boost from the proposed MSW neutrino oscillation solution to the solar neutrino problem, together with the seesaw mechanism for neutrino mass generation. An astrophysical solution is difficult to reconcile with the combination of Gallex, Sage, Homestake and Kamiokande data. (However, the Gallex result is only about 2σ from the standard solar model.) Although ν-dominated adiabatic models are strongly ruled out by CMB limits, ν's are the best dark matter for cosmic string models, and CDM models with a moderate fraction ($\Omega_\nu \sim 0.1$–0.3) of light neutrinos give one of the nicest explanations of large scale clustering data in the post-COBE era (§5,6).

t_0: Renzini [3] gives (13–15)$\pm$3 Gyr for globular cluster ages, with the biggest uncertainty (20–25%) coming from the distance modulus, and with smaller uncertainties from metallicity, helium diffusion, *etc.* Nuclear cosmochronology is more uncertain, with ages of the oldest heavy elements anywhere from 10 to 20 Gyr being possible. The age of the Milky Way disk from white dwarf cooling and open cluster ages is about 8–10 Gyr. To these one must add estimates for formation times. A 15 Gyr age for a universe with $\Omega \approx 1$ in cold matter and baryons — as in the 'standard CDM model' — would require a Hubble constant below 45; $H_0 = 65$ requires a 10 Gyr total age.

H_0: All of the 'astronomically-calibrated' methods to determine distance give, according to most practitioners (*e.g.,* Tonry [4]), values of H_0 around 80. What is rather compelling is not each method by itself, but the consistency of the result from Tully-Fisher distances (84 ± 10), planetary nebulae (80 ± 10) and galaxy surface brightness fluctuations (80 ± 10). Methods based on 'physics' tend to give lower values. If Type Ia supernovae are standard candles, they give $\sim 50 \pm 10$ (*e.g.,* Sandage *et al.* [5] calibrated SNIa with a Cepheid in a distant galaxy using the Hubble Telescope and got 46). Kirshner *et al.* [6] quote 60 ± 10 for the Baade-Wesselink (moving photosphere) method for Type II supernovae, but their distances are consistent with those obtained for individual objects using the 'astronomy' methods. The Sunyaev-Zeldovich effect is the upscattering of CMB photons from hot gas via Compton scattering off the electrons. Because different

lines of sight in the Universe penetrate different hot gas histories, anisotropies in the background radiation result with a characteristic spectral signature that allows one to separate them from other sources. Combining Sunyaev-Zeldovich and X-ray observations of clusters (with all of the uncertainties that that entails) allows one to estimate the Hubble constant; the best observed cluster for this, Abell 665, gives the theoretically happy $H_0 = 40 \pm 9\,\mathrm{km\ s^{-1}\,Mpc^{-1}}$ (Birkinshaw *et al.* [7]), but SZ/X estimates of H_0 have always been on the low side. Gravitational lensing time delays have tended to give low H_0 but the modelling uncertainties are great.

$[H_0t_0](\Lambda,\Omega)$: Even with nonzero Λ or negative curvature, $H_0 > 70$ and a 15 Gyr age lead to a devastating conclusion for cosmology. To emphasize this we show what happens to ages when we take the density in nonrelativistic matter ($\Omega_{nr} = \Omega_B + \Omega_{cdm}$) to be 0.2 and take Ω_Λ to be 0.8. $H_0 = 100$ gives 11 Gyr, $H_0 = 80$ gives 13.5 Gyr and $H_0 = 70$ gives 15 Gyr. For these H_0, open universes with $\Omega = \Omega_{nr} = 0.2$ give 8.5 Gyr, 11 Gyr and 12 Gyr, respectively. Although it is possible to reconcile the high H_0 with lower Ω_{nr}, (0.1 with $\Omega_\Lambda = 0.9$ gives 16 Gyr for $H_0 = 80$), the amount of clustered dark matter appears to be in excess of 0.2, and Λ-energy does not cluster. Intermediate values for H_0t_0 can be obtained if there is a form of matter present whose equation of state results in a slower density falloff, intermediate between the $\sim a^{-2}$ falloff of curvature energy density and the $\sim a^0$ falloff of cosmological constant energy density, with a the expansion factor. Any decline slower than $\sim a^{-3}$ requires that the pressure of such matter be negative, but this is possible if potential energy dominates over kinetic, and is realized, for example, with scalar fields, and, indeed, is a prerequisite for inflation.

Cosmic Coincidences: As Dicke and Peebles have emphasized, to have nonzero Λ or nonzero curvature becoming dynamically important just at the present epoch would involve a remarkable coincidence, but we have learned to live with other apparent coincidences, *e.g.*, the nearness of the epochs of recombination and of the transition from radiation to matter domination; and the similarity of the dark matter and baryon densities. Anthropic arguments that restrict the values of Ω and Λ so humans can exist (*e.g.*, requiring a matter-dominated epoch to ensure sufficient perturbation growth) make most physicists cringe. Still, one might argue that a molecular life selection function has been applied to at least one of the set of all possible accelerated patches that underwent reheating.

Ω: The argument that if our Hubble patch is part of a much larger region of space that inflated its mean curvature would be nearly unity is quite compelling. Curvature is a combination of a squared gradient and the Laplacian acting on a large scale gravitational potential, a unified picture within which to view curvature fluctuations and the curvature mean. Thus I consider the tininess of fluctuations in the curvature on scales around H_0^{-1}, as shown by COBE, to strongly suggest that the mean curvature will also be tiny. Otherwise we need a spatial cosmic coincidence, a great increase in amplitude for wavelengths beyond $H_0^{-1}|1-\Omega|^{-1/2}$ (something that *e.g.*, double inflation could in principle give however). The traditional mathematical picture of a smooth expanding ball(oon) or saddle of constant mean curvature with tiny ripples of unrelated origin added as an afterthought was the historical approach, but it seems contrived to me. In any case Ω doesn't do nearly as well as Λ in solving the H_0t_0 problem.

Λ: Before embracing a Λ-dominated cosmology, with density parameter $\Omega_\Lambda \equiv \Lambda/(8\pi G\bar{\rho}_{crit})$ in excess of 1/3, we should recall that the Steady State theory was a deSitter space theory with nonzero Λ. But if we are now in a (new) period of accelerated expansion, there are no prospects for a reheating episode like the one that must have ended the last period of inflation, if indeed there was one: no ongoing matter creation *a la* Hoyle *et al.*, just a 'cold death' of the Universe. Nonzero Λ does help explain the LSS (§6).

A nonzero mean scalar field with vacuum (potential) energy density $\langle V(\phi)\rangle = (3\times 10^{-12}\mathrm{Gev})^4\Omega_\Lambda h^2$ can be a superposition of very long ULSS waves — unlike curvature energy it involves no gradient. The physics case against Λ is well known: whatever particle scale we refer it to, this density is tiny; *e.g.*, in Planck energy density units ($m_p^4 \sim 10^{94}\mathrm{gm\,cm^{-3}}$), we have $\langle V(\phi)\rangle \lesssim 10^{-122} m_p^4\Omega_\Lambda h^2$. The 'vacuum' energy density is also expected to renormalize its value during the cooling of the universe (before the first three minutes). Thus, it is not only hard to understand why the effective Λ is so small now, but even if it is zero we really have no idea why it should be so — even with Euclidean wormhole physics. Since inflation relies on a large effective Λ generated by the inflaton field to drive the accelerating expansion (*e.g.*, $\langle V(\phi)\rangle \sim (10^{16}\mathrm{Gev})^4$ in chaotic inflation when LSS waves were generated), we should not be too surprised if inflation and its Zeldovich density spectrum are modified when the Λ problem is finally solved.

Nonzero Λ or vacuum energy can also be viewed as just another form of dark matter; for that matter, so can curvature energy, $\Omega_{curv} \equiv 1-\Omega$.

3. Theories for the Initial Fluctuations Within our Hubble Patch

Quantum Noise: The main paradigm after a decade remains the inflation one, with quantum zero point oscillations of scalar fields providing the source of adiabatic (curvature) fluctuations. In the standard stochastic inflation picture, most of the *original* volume that got into acceleration would have passed into deceleration, accompanied by particle production, and eventually a candidate domain for the bit of the Universe that we see, although by far the largest current *physical* volume in the universe would still be undergoing acceleration. A $\lambda\phi^4$ potential invoked in chaotic inflation would need $\lambda \sim 10^{-13}$ in order that the quantum noise satisfies CMB observations. Such a tiny λ is unnatural since, even if one began with such a small coupling, it would generally become

far larger through radiative corrections. There have been many attempts to construct models with natural, stable, small effective couplings; *e.g.,* 'natural inflation' in which the inflaton is the phase of a complex field with a radiatively-protected effective λ of order $(m_{GUT}/m_P)^4$, where $m_{GUT} \sim 10^{16}$ GeV is the GUT energy scale and $m_P \sim 10^{19}$ GeV is the Planck mass [8,9].

Power Law Breaking of Scale Invariance: Exact scale invariance (*i.e.,* $n_s = 1$, where the initial *rms* density perturbations are $d\sigma_\rho^2(k)/d\ln k \propto k^{3+n_s}$) cannot occur in inflation. Most models give approximate power laws with n_s below unity, but not by much. This gives a little more power in LSS and VLSS bands. To get more complex spectra (mountains, valleys, plateaus) a spatial cosmic coincidence must be built into the potential surface of the scalar fields that drive inflation, or special (very unlikely) initial conditions must be invoked for our patch (*e.g.,* Salopek *et al.* [10] and references therein). This is distasteful, but all our VLSS, LSS and MSS observations probe the structure of only a tiny section of the scalar field potential surface.

Isocurvature Baryon Perturbations: What is difficult to arrange in inflation models is less power than scale invariant spectra give. This and the requirement that the dark matter would be purely baryonic (in spite of the $\Omega_B \lesssim 0.064\,(2h)^{-2}$ nucleosynthesis limit) are the main reasons for not taking those special isocurvature baryon models that are able (maybe) to reproduce the cosmic structure we observe very seriously. These models have initial fluctuations in the baryon number, but no net fluctuation in the curvature, so are orthogonal to the usual adiabatic modes (that *e.g.,* the standard CDM model presupposes). Nearly scale invariant isocurvature spectra are very strongly ruled out by CMB constraints. (At least one particle-physics motivated model exists in which scale invariance on small scales goes over to the observationally required white noise spectrum on large scales, but a cosmic coincidence is required for the transformation scale.)

Topological Defects: In spite of inflation's ability to smooth our Hubble patch and generate fluctuations through quantum oscillations, there is a healthy scepticism that it is the only path to cosmic smoothness and that the inflaton potential will have just the right coupling to give the 'observed' perturbations. Among searches for alternative generation mechanisms, topological defects in field configurations formed during cosmological phase transitions have been the most promising. In spite of field smoothing through gradient interactions and radiative losses once there is causal contact, these field defects do last long enough to generate matter density perturbations before disappearing. Examples are the 1D cosmic strings and the 3D 'global' monopoles and textures; 2D domain walls do not lead to viable models.

Defect models generate approximately scale invariant initial fluctuations, but these are decidedly non-Gaussian and so have unique features for galaxy formation: in particular, some objects can form shortly after recombination and result in early reionization of the Universe, which could lower small angle CMB anisotropies below observability.

Constraints on Explosion-induced Structure: Explosion-driven or radiation-pressure-driven structure formation, amplifying small seed fluctuations, would release more 'y-distortion' energy through Compton cooling of electrons than the current strong FIRAS limits allow – at most 0.01% of the total energy in the CMB at the 95% confidence limit (Mather *et al.* [1]). Nonetheless local explosions and radiation forces still have lots of room to locally amplify (or deamplify) structure over the UMSS, VSSS, SSS and even MSSS bands.

4. Cosmic Structure Probes

In Figure 1(a), we show the wavebands probed by various large scale structure observations (large scale streaming velocities LSSV, the angular correlation of galaxies $w_{gg}(\theta)$, the power spectrum and redshift space correlation function of galaxies as probed by the QDOT redshift survey, the correlation function of clusters of galaxies ξ_{cc}). The best indicator for large scale power is the angular correlation function of galaxies.

The range covered by these LSS probes should be contrasted with the range covered by microwave anisotropy experiments, each of which can be well characterized by filters which act upon a 'power spectrum for $\Delta T/T$ fluctuations' (see Bond and Efstathiou [11] for a precise definition). Filter functions are shown for the COBE (7° beam) DMR experiment [12,13], the MIT (3.8° beam) balloon experiment of Page *et al.* [14], the UCSB 1991 South Pole (1.5° beam) experiment of Gaier *et al.* [15] and Schuster *et al.* [16], the UCSB 1989 South Pole (0.5° beam) experiment of Meinhold and Lubin [17] and the Caltech OVRO (1.8′ beam) experiment of Readhead *et al.* [18]. The balloon-borne UCB/UCSB MAX and Goddard/MIT experiments have filters which cover about the same range as the SP89 experiment and there is a new Caltech experiment planned to cover the region between SP89 and OVRO.

Thus CMB anisotropy experiments cover the entire VLSS and LSS bands. Below $\sim 5\,h^{-1}$Mpc, *primary anisotropies* of the CMB (those one calculates from linear perturbation theory and which are easiest to interpret) are basically erased if hydrogen recombination is standard (SR line in Fig. 1), so photons decouple from baryons at $z \sim 1000$ and freely stream to us; if there is an early injection of energy which ionizes the medium, photon decoupling would not have occurred until a lower (Ω_B-dependent) redshift and would erase $\Delta T/T$ power on scales typically below the NR (no recombination) line shown.

The light long-dashed filter curves at smaller scales show the regions of the spectrum probed by the VLA, by the SCUBA array on the sub-mm telescope JCMT, by the IRAM mm-dish, and by the OVRO mm-array. Although their beams are too small to see primary CMB anisotropies, they will provide invaluable probes of *secondary anisotropies* (those generated by nonlinear effects, including redshifted dust emission from galaxies and Thomson scattering from

Figure 1: *(a) Cosmic waveband probes; (b) density power spectra; (c) galaxy power spectra.*

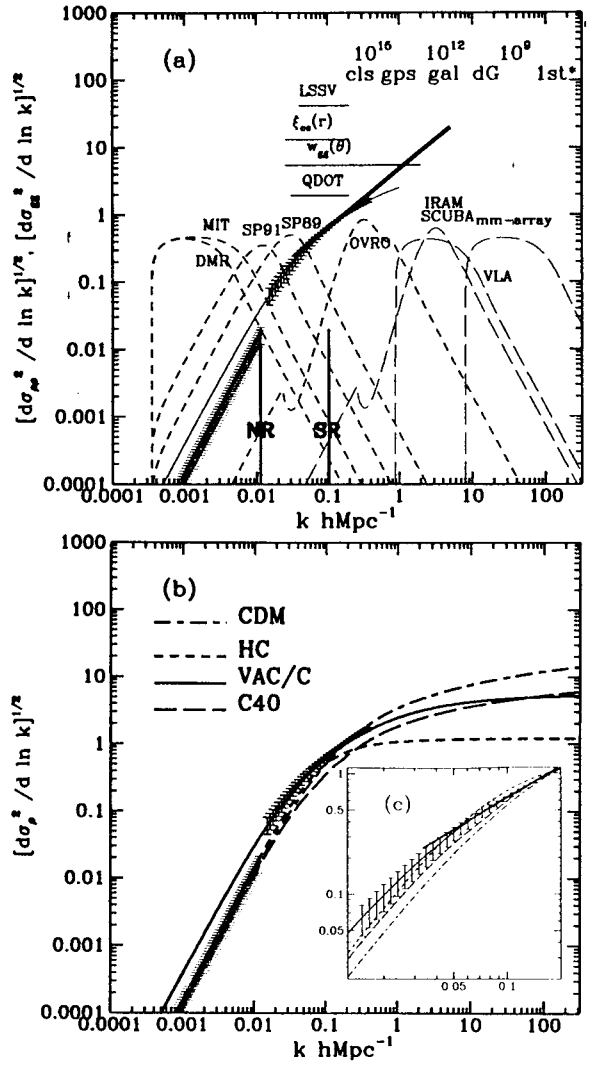

nonlinear structures in the pregalactic medium.)

'Observed' power spectra (actually their square roots) are shown as hatched regions for density fluctuations inferred from COBE and for galaxy fluctuations inferred from the APM and ROE w_{gg} data (Maddox *et al.* [19], Collins *et al.* [20]). The long wavelength hatched curve is the DMR-normalized scale invariant spectrum (assuming an $\Omega_{nr} = 1$ model, and including a 30% error budget). The heavy curve extending the hatched w_{gg} power into smaller distances is the power corresponding to the well known $\xi_{gg}(r) = (r/r_{0gg})^{-\gamma}$ 3D correlation function form, where the CfA1 redshift survey values have been taken, $r_{0gg} = 5.4\,h^{-1}$Mpc and $\gamma = 1.8$. Power spectra derived from the QDOT (Kaiser *et al.* [21]), IRAS 1.2 Jansky (Fisher *et al.* [22]) and CfA2 (Vogeley *et al.* [23]) redshift surveys are compatible with the range inferred from w_{gg} when account is taken of redshift space distortions and a possible clustering offset between IRAS and optically identified galaxies. Remarkably, cluster-cluster correlations also seem to be compatible with this spectrum (Dalton *et al.* [24], Nichol *et al.* [25]), as do galaxy-cluster cross correlations (Efstathiou [26]).

Power spectra for gravitational potential fluctuations are related to those for the density through the Poisson-Newton equation $\nabla^2\Phi = 4\pi G a^2 \delta\rho$; thus they are flat for scale invariant spectra on large scales ($d\sigma_\Phi^2(k) = k^{-4} d\sigma_\rho^2(k)$ $\propto k^{n_s-1} d\ln k$). Power spectra for large scale streaming velocities are related to those in density though the continuity equation, ($d\sigma_v^2(k) = k^{-2} d\sigma_\rho^2(k) \propto$ $k^{n_s-1} d\ln k$).

The power spectra for primary $\Delta T/T$ fluctuations are more complex than these, because they include effects associated with geometrical ripples in the past light cone (Sachs-Wolfe effect), with the flow of electrons at photon decoupling, the degree of photon compression at decoupling, and the damping associated with the width of decoupling mentioned above.

In Figure 1(a), we also show the band of waves whose local constructive interference leads in time to collapsed virialized dark matter condensations of the type shown. Of course, such a characterization presupposes that there are waves of significant amplitudes to form the structures. This will generally be true for hierarchical models, in which the *rms* power in density fluctuations in each waveband is monotonically increasing with decreasing scale. However, damping processes or tilted initial spectra may require some of the shorter distance structure to arise from fragmentation and other non-gravitational effects.

In Figure 1(b), linear density-density power spectra normalized to the COBE DMR data are compared with the galaxy data for the models defined by Table 1 in §5. The notation for the models is that of Bardeen *et al.* [27], hereafter BBE. To translate into galaxy-galaxy power spectra to match the second hatched region, it is usual to multiply by a single constant biasing factor for the galaxies in question. There are so many orders of magnitude in the Figure that the LSS 'extra power' problem is not that evident, a strong indicator that nearly scale invariant spectra may be on the right track. The insert Figure 1(c) gives a closeup of the galaxy clustering regime, with the (linear) biasing factor $b_g = \sigma_8^{-1}$

now included (see §5.1). This shows that the shape of the CDM spectrum does not agree with the LSS power. Scale dependent biasing which suppresses power on small scales could be one way out (Couchman and Carlberg [28]). However the other models in Table 1 can explain the LSS power, although, like CDM, each has at least one Achilles' heel that may be fatal.

5. COBE-normalized Fluctuation Spectrum Amplitudes

For a given cosmological model, the shape of the (linear) density fluctuation spectrum is fixed, but the overall amplitude is arbitrary. The shape depends upon the initial spectrum (*e.g.,* characterized by a local spectral index $n_s(k)$) and by its evolution as the waves re-enter causal contact in the post-inflation era, which makes the linear spectrum a function of H_0, Ω, Ω_B, and the type and amount of dark matter present. COBE's detection can be used to normalize the spectrum, as is described in §5.2. First we introduce besides the standard cold dark matter model, three inflation-based variants that are contenders in the post-COBE era for *the* structure formation theory.

5.1 Spectral Amplitudes for Post-COBE Models

To discuss differences that these models give over the various waveband realms, we characterize the amplitude in the bands by relative *rms* fluctuations in the mass in spheres of radius R (in $\mathrm{h^{-1}Mpc}$), *assuming linear growth of perturbations*: $\sigma_R \equiv (\Delta M(<R)/\bar{M})_{rms}$. The average mass initially within the sphere is related to R by $\bar{M} \approx 10^{12.4}(R/\mathrm{h^{-1}Mpc})^3\,\mathrm{M_\odot}$.

It has become standard to characterize the amplitude of primordial fluctuations by σ_8. The radius $R = 8\,\mathrm{h^{-1}Mpc}$ roughly divides LSS from MSS. The observed *rms* fluctuations in the galaxy distribution are unity on this scale, but this includes nonlinear and galaxy biasing effects. If the dynamics is sufficiently linear on this scale, then to agree with the unity observation, the mass fluctuations would have to be amplified by a factor $b_g = \sigma_8^{-1}$. Thus σ_8^{-1} has come to be known as the biasing factor. However, nonlinear effects could lead to smaller amplifying factors, differences between galaxy types could imply different biasing factors and complexities associated with the formation and merging of bright galaxies and other gastrophysical processes could make the biasing factors functions of environment and of scale. σ_R scales with the normalization σ_8.

Typical values of COBE-normalized σ_R's for the different bands are shown in Table 1 for some popular post-COBE models of structure formation. All models but one have an initially scale invariant ($n_s = 1$) adiabatic spectrum. CDM denotes the standard model with $H_0 = 50$, $\Omega_B = 0.05$, $\Omega_{cdm} = 1 - \Omega_B$. A high σ_8 CDM model has problems explaining the relatively quiescent pair velocities of galaxies on small scales, and overproduces rich clusters (§6).

The redshift $z_{nl}(R)$ at which an *rms* perturbation of scale R reaches unity, assuming a linear extrapolation of the density evolution, is simply $1 + z_{nl}(R) = \sigma_R$ for CDM Universes, since $\sigma_R \propto$ the scale factor a. (Recall that $\delta\rho/\rho \sim a \sim t^{2/3}$ is the growing mode for density perturbations in a matter-dominated universe.) $z_{nl}(R)$ provides a first (somewhat low) estimate for when dark halos of mass $\bar{M}$ form in abundance (a few % of the mass will be in such halos at $1 + z \sim 1.4\sigma_R$).

Table 1: Characteristic Density Fluctuation Levels

realm	probes	$[\Delta M/M]_{rms}$	CDM	VAC/C	HC	C40
ULSS	'global'		0	0	0	0
VLSS	COBE	σ_{300}	$0.005\sigma_8$	0.012	0.006	0.004
LSS	$w_{gg}, P_{gg}(k)$ $\xi_{cc}, \xi_{cg}, v_{bulk}$	σ_{25}	$0.3\sigma_8$	0.37	0.27	0.19
MSS	cls	σ_8	0.94	1	0.7	0.6
	gps	σ_4	$1.8\sigma_8$	1.6	1	1.0
SSS	gals, QSOs	$\sigma_{0.5}$	$6\sigma_8$	4.3(6)	1.8	3.1
VSSS	dG, Ly α	$\sigma_{0.1}$	$11\sigma_8$	6.8(9)	-	5.2
USSS	1st stars	$\sigma_{0.01}$	$21\sigma_8$	10(14)	-	9
FLAW			w_{gg}	v_{bulk}	z_{gf}?	H_0, v_{bulk}

Other models shown in the Table are: VAC/C, a $\Lambda \neq 0$ model with $H_0 = 80\,\mathrm{km\ s^{-1}\,Mpc^{-1}}$, $\Omega_\Lambda = 0.75$ and $\Omega_{cdm} = 0.25$. For Universes with $\Lambda \neq 0$, σ_R evolution slows down once Ω_Λ dominates, so $1 + z_{nl}(R)$ will be higher than σ_R; we list these in brackets after the σ_R values when the difference is significant.

HC is a mixed hot and cold dark matter model, with $\Omega_\nu = 0.3$ in light massive neutrinos ($m_\nu = 7$ ev) and $\Omega_{cdm} = 0.7$ in CDM (van Dalen and Schaeffer [29]). In BBE [27], it was argued that HC models with significant ν content would not form galaxies early enough, based upon an $\Omega_\nu = 0.4$ ($m_\nu = 10$ ev), $\Omega_{cdm} = 0.5$, $\Omega_B = 0.1$ HC model, but it was also shown that it would give LSS correlations and flows within the current observational range. The HC model in the Table is not quite as bad, but $\sigma_{0.5}$ may still be too small; however, one can roughly match the LSS data with Ω_ν as low as ~ 0.1 ($m_\nu \approx 3$ ev). Thus HC shows much promise. N-body studies support these conclusions by Davis *et al.* [30], and Klypin *et al.* [31] basically support these conclusions.

C40 is a CDM model, but with $H_0 = 40$. It also has a slight spectral index change, $n_s = 0.95$ as suggested by chaotic inflation, and has $\Omega_B = 0.1$, the nucleosynthesis upper limit for $H_0 = 40$. All of these effects conspire to give just about enough LSS.

For cosmic string, monopole and texture models, the COBE-inspired value for σ_8 would have to be below 0.3 or so (Bennett, Bouchet and Stebbins [32], Bennett and Rhie [33], Pen, Spergel and Turok [34]). It will not be easy for defect proponents to concoct a viable model for structure formation and LSS

flows with such an amplitude, although more detailed simulations are needed to decide. (Remarkably, the cosmic texture model in an $H_0 = 50$ CDM universe seems to give a power spectrum with the same shape as that inferred from LSS clustering observations [35].)

There are other inflation-based models which can reproduce the LSS. The standard CDM model could explain the large scale clustering data if $0 < n_s < 0.6$, but the COBE data implies such low primordial amplitudes that galaxy formation would occur too late to be viable if $n_s < 0.6$, and the large-scale galaxy velocities would be too small if $n_s < 0.7$, as Adams *et al.* [9] showed. If gravity waves contribute to the DMR signal, as they are expected to do in power law models such as extended inflation and inflation with exponential potentials (but not in natural inflation which also predicts power laws), $n_s > 0.8$ is required.

A CDM model with a 17 keV neutrino which decays (without significant photon emission) in a year or so would give the required extra power (Bond and Efstathiou [36]), but it gives such a low σ_8 ($\lesssim 0.4$) that galaxy formation will occur too late and cluster abundances can't be matched. Of course much of the motivation for considering decaying neutrinos with masses in the keV range was considerably diminished with the experimental demise of Simpson's 17 keV neutrino.

5.2 Statistical Significance of CMB Anisotropy Detections and σ_8

5.2.1 DMR Likelihood

The strength of the detection is indicated by the likelihood curve shown in Figure 2 for the standard CDM model. (This is based on a Bayesian treatment of the '90 A+B X 53 A+B' correlation function data given by Smoot *et al.* [12] and assuming a Gaussian distribution of errors and using a uniform weight all sky approximation to treat the theoretical variance in $C(\theta)$.) The relation between σ_8 shown here and the value of the *rms* quadrupole used to normalize the angular power spectrum that the DMR team uses is $Q_{rms,PS} = 14.9\sigma_8\mu K$, which gives a maximum likelihood value of $14\mu K$. With the Bayesian analysis used here, there are about 15% errors (at the one sigma level) on the normalization σ_8. Seljak and Bertschinger [37] also use a likelihood approach on the correlation data to derive a value similar to the one I get for $Q_{rms,PS}$. The DMR team derive $15.3\mu K$ for this '90 A+B X 53 A+B', 9% larger than that given here, with bigger error bars on their effective σ_8, and actually adopt the larger value of $17\mu K$ for a scale invariant spectrum based upon the analysis in the Wright *et al.* [13] paper. If I do a similar analysis on the Wright *et al.* rather than the Smoot *et al.* correlation function, I get a value only about 5% higher, but it is sensitive to whether I exclude angular bins in the correlation function or not. The difference between their result and that shown here might be explained in part by the influence of Galactic cuts, by their use of uncorrelated chi-squared rather than Bayesian statistics and correlation function differences from DMR map to DMR map.

Figure 2: *DMR, MIT, SP91 likelihood functions for a standard CDM model.*

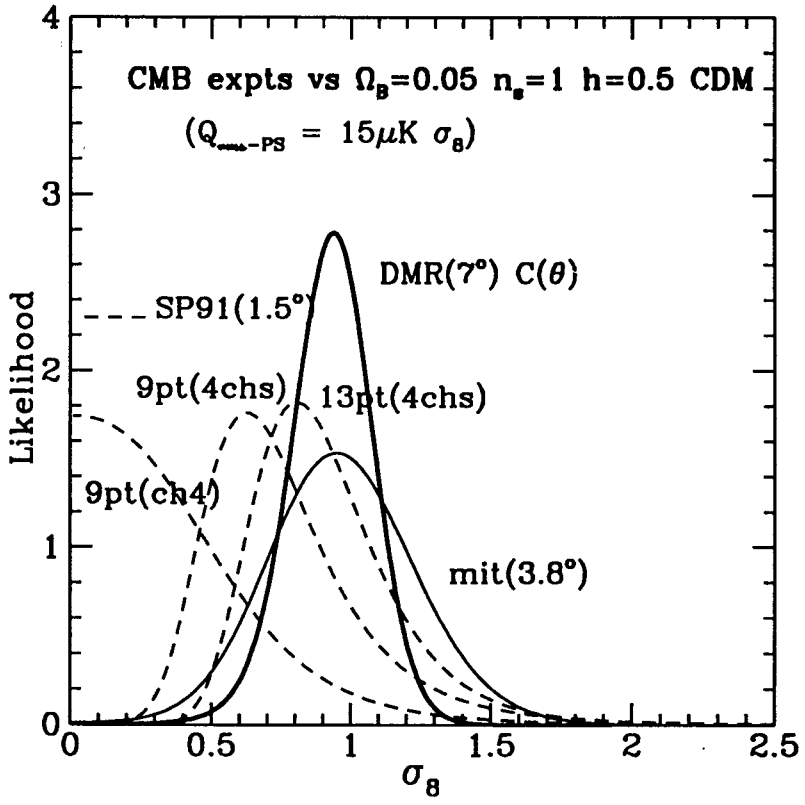

The correlation function value compares with the value I derive using the *rms* anisotropies in 10° patches given by DMR: $Q_{rms,PS} = 14.3\mu K$, *i.e.*, $\sigma_8 \approx 0.96$, about the same as the correlation analysis gives but with a 20% error compared to 15%. Wright (private communication) points to the role Galactic cuts may have in increasing the value; he gets $17\mu K$.

5.2.2 DMR Quadrupole

The DMR team give the five quadrupole components with error bars and claim the squared-quadrupole $Q^2_{rms,OBS}$ on the sky is $(13.4 \pm 5\mu K)^2$ (Bennett *et al.* [38]). Gould [39] suggested that the quadrupole (but he meant $Q_{rms,PS}$ not the observed one) was smaller, about $9\mu K$, and that $Q_{rms,PS} = 0$ was a statistically significant possibility. He also criticized the method of error estimation used by the DMR team.

I have used Bayesian likelihood methods to address the statistical significance of the $Q_{rms,OBS}$ detection and how useful the quadrupole data is by itself in determining $Q_{rms,PS}$. I assumed that the quoted error bars on each of the components were Gaussian standard deviations, although these encompass both a statistical and a systematic component, and the latter would have a non-Gaussian distribution. However the split is not available from the Smoot *et al.* papers. In any case, the Gaussian assumption probably leads to a worse story for the quadrupole than a careful analysis of the true data would give.

The distribution functions for the observed quadrupole $Q^2_{rms,OBS}$, found by FFT inversion of a characteristic function, were highly skewed and broad, but quite compatible with the DMR amplitude of $13 \pm 5\mu K$. For the 'reduced Galaxy' data, I get $13.4^{+4.6}_{-7.5}\mu K$ for a Galactic cut of 20° and $12.6^{+4.2}_{-6.7}\mu K$ for a Galactic cut of 10°; the DMR team got $13 \pm 5\mu K$ and $13 \pm 4\mu K$, respectively. For the 53 GHz map with a 20° cut, I get $10.7^{+2.9}_{-4.1}\mu K$, whereas the DMR team got $11 \pm 3\mu K$.

If for the estimate of $Q_{rms,PS}$, I adopt the median of the Bayesian probability curves (with a linear prior probability in $Q_{rms,PS}$), then I get 11.1, 10.3 and 11.0 μK for the three cases listed above, respectively. The 53 GHz, 20° cut, 1 sigma (*i.e.*, 68% probability) region is $11.0^{+7}_{-4.8}\mu K$, with a maximum of the likelihood at $9\mu K$, in agreement with Gould's χ^2 estimate, but with mean at $13\mu K$. With only five degrees of freedom in the Bayesian analysis, the results are somewhat sensitive to the choice of prior probability, *e.g.*, a quadratic prior always gives higher values, and a logarithmic prior always gives unrealistically low ones. A recommended prior that is invariant under change of measure is Fisher's noninformative prior, which gives $10.0^{+6}_{-3.9}\mu K$, so I believe the linear prior results to be quite robust. The most probable, median and mean translate to $\sigma_8 = 0.64, 0.74, 0.87$, respectively, more compatible with my correlation function σ_8 than the value the DMR team gives, but still slightly low. However the broadness of the likelihoods mean that $Q_{rms,PS}$ derived from the quadrupole data is fully compatible with the $Q_{rms,PS}$ determined from the correlation function.

5.2.3 Effects Lowering σ_8

While the Wright *et al.* analysis may cause σ_8 to be up to 20% higher than the values shown in the Table, there a number of physical effects which will lower the value. Effects associated with the gentle breaking of scale invariance which bring the spectral index of the fluctuations below $n_s = 1$, the influence of gravity waves on large angle anisotropies, and H_0 and Ω_B modifications all cause σ_8 to decrease. For a fairly conservative inflation model, (chaotic inflation with a $\lambda\phi^4$ potential), the spectral index in the VSS to LSS regime is 0.95, lowering σ_8 by 10%; gravity waves further lower it by 10% (Starobinsky [40], Abbott and Wise [41], and a plethora of post-COBE papers cited in [9]); using $\Omega_B = 0.05$ indicated by primordial nucleosynthesis gives a further lowering to $\sigma_8 = 0.75$. Models with n_s even smaller are certainly possible in inflation and lead to even more drastic modifications. Lowering H_0 to 40 yields a further 30% lowering. Thus decreases of at least 25% are quite plausible over the naive COBE-normalized σ_8. On the other hand, there are many inflation models which can give n_s quite close to unity and there are some with negligible gravity wave corrections, so we must currently live with combined uncertainties of about 30% in σ_8, for 'standard inflationary models.' This is not that much better than the constraints we had before DMR's observation, just based upon the ability of the models to form the structure we observe; but, of course, now with DMR the inflationary models have increased weight. Further, the observational error bars on DMR can go down a factor of 2 when all four years of data are analyzed.

Whatever the final resolution of the specific amplitude, the *strength* of the detection shown by the likelihood function of Figure 2 will surely survive.

5.2.4 MIT Likelihood

Also shown in Figure 2 are the likelihood curves for the MIT balloon experiment (with a beam half the size of COBE's) flown by Cheng, Page and Meyer [14]. It has four frequency channels, two for monitoring Galactic dust (440μ 633μ) and two for the primary CMB signal (1149μ adn 1786μ). The balloon arced out six rings on the sky over its five hours of integration, with the smallest error bars in the patches where the rings overlapped. The map is therefore highly complex compared with the DMR all sky maps, although they too are inhomogeneously sampled. Nonetheless it contains information on all of the multipoles larger than the scale of its Gaussian beam ($L_{beam} \approx 35$, *c.f.* DMR's $L_{beam} \approx 19$). There are about five hours of data in the MIT map and one year in the DMR map. The reason that the MIT experiment can be competitive is that its Helium-3 cooled bolometers are much more sensitive than the passively cooled (non-cryogenic) radiometers used on COBE. So far only one frequency channel (1786μ, *i.e.*, 168 GHz) has been used in the detailed data analysis. There is also another MIT balloon flight that has yet to be analyzed.

I have been analyzing the MIT data using the Bayesian approach on the complete map, which is preferred over the correlation function approach which

reduces the full map information to only certain quadratic combinations of the pixel values. The detection is at *exactly* the level COBE sees, with a 27% one sigma error. This is a recent result, but earlier analysis using angular correlation functions and a certain quadratic statistic that I have shown is the best quadratic measure of the anisotropy amplitude (called the Boughn-Cottingham statistic in the trade) indicated a detection as well, but because these reduce the full map information, the error bars were larger. The full-map likelihood calculation requires monopole and dipole subtractions and frequent inversions of N^2_{pixel} matrices, with $N_{pixel} \sim 3500$. An eigenvector analysis proved to be the least computationally expensive method to do this and moreover led to the very useful concept of orthogonal signal-to-noise modes for the map. Power spectra constructed for these modes clearly showed that a spurious white noise component existed in the data that had nothing to do with large angle power on the sky. (It only contributes to the zero angle bin in correlation function analysis and the Boughn-Cottingham measure effectively filters it out, so those earlier detection indications were fine). The best way to analyze the data is to construct a joint probability distribution in cosmic signal amplitude and white noise amplitude. The likelihood contours were concentrated around a sharp maximum that had nonzero amplitudes for the cosmic signal and white noise (ratio about 1 to 2.5), with zero in white noise excluded at more than the 10 sigma level and zero in cosmic signal excluded at more than the 3 sigma level. The likelihood plotted in Figure 2 is actually the marginal distribution in signal amplitude, found after integrating the joint distribution over all possible white noise amplitudes.

A positive cross-correlation of the MIT map with the DMR maps has recently been reported by Ganga, Page, and the DMR team members [42], indicating that both experiments are seeing the same pattern of bumps on the sky and also indicating that the signal amplitudes cannot be too dissimilar. Combined with the more exact measure of amplitude compatibility shown by the likelihood functions, this result allows us to conclude that what the DMR and MIT experiments are seeing really exists on the sky rather than being instrumental or spacecraft/atmospheric in origin, and also that the bumps are consistent with a thermal spectrum, since the experiments probe quite different wavelengths (30, 53, 90 GHZ for DMR, 170 GHz for MIT) but the amplitudes are about the same.

Although the DMR and MIT curves are plotted against σ_8 for the specific CDM model shown, the same agreement will exist for any scale invariant model, except the value of σ_8 will differ, as in Table 1. (A caveat here is that NR models will give slightly different answers for DMR and MIT, but the errors are large enough to accommodate them.)

5.2.5 South Pole 1991 Likelihood

Smaller angle experiments such as the SP91 experiment are sensitive to the details of the cosmological model, in particular the value of Ω_B, since they probe gas flows at the time of recombination as well as the gravitational potential fluctuations that the larger angle experiments probe. It is unclear at the present time how to interpret the anisotropies that are now observed in this and other intermediate angle experiments, since the primordial signal may be contaminated by Milky Way or extragalactic sources, especially by synchrotron radiation at lower frequencies and Galactic dust emission at higher frequencies. The data which has been analyzed for SP91 so far consists of one 9 point scan of the sky (Gaier *et al.* [15]) and one 13 point scan of a different region (Schuster *et al.* [16]), each in four channels centred around 30 GHz. If contamination exists it is more likely to be from synchrotron sources than from dust at these frequencies. The SP91 likelihood functions of Figure 2 are calculated assuming that the only signal is a cosmic primary $\Delta T/T$ signal from the scale invariant CDM model of Table 1. When all four channels are analyzed simultaneously, both scans give a maximum to the likelihood, but if channel 4 of the 9 point scan is analyzed alone, there is no maximum – indicative of no signal, but within large statistical errors. The all-channel likelihood functions get substantially broader than those shown if we add a simplified synchrotron radiation signal of Gaussian-distributed white noise with an angular 'coherence angle' optimally-sized to take away as much of the signal as possible from the primary $\Delta T/T$. Calculating the marginal distribution in the cosmic signal amplitude by integrating over the synchrotron amplitude in the same way that the MIT white noise was integrated away, I find a maximum to the distribution remains in the 13 point data, within 1 sigma of DMR, but disappears in the 9 point data, with a 10% chance of having the COBE detection level (which is only a little above 1 sigma above the median). At this point I think that all we can say is that the likelihood contours for these two scans are not clearly inconsistent with the CDM model or with the other models of Table 1 (Bond and Efstathiou [43]). However, the next year or so will be very exciting as more high precision anisotropy data probing a variety of resolution scales come in to show us whether we are converging upon a specific cosmological model.

6. LSS Probes of the Fluctuation Spectrum

The best information on large scale structure comes from the angular galaxy-galaxy correlation function rather than from redshift surveys. If the act of forming galaxies does not build in a large length scale to the correlations, then w_{gg} will tell us about the shape of the underlying (dark) mass distribution which defined the gravitational instability process. Current ideas of formation allow an arbitrary uniform 'biasing factor' which is the ratio of the galaxy density to the mass density smoothed over a large scale. However, it is by no means clear that galaxy formation will not suppress the power on smaller scales because of processes such as merging. Thus, without other evidence one could argue that using galaxies to measure the primordial spectrum is flawed. The data with uniform biasing factor is described in §6.1.

Theorists have long dreamed that clusters of galaxies were simple deep potential wells, nicely virialized, relatively isolated and spherical, with a uniform temperature T_X, dark matter velocity dispersion v_{DM}, and galaxy velocity dispersion v_g all simply reflecting the binding energy per mass of the beasts. If so, then they are easy to model theoretically. Their clustering properties would be proportional to that of the underlying (dark) mass distribution on large scales, so the cluster-cluster correlation function should directly tell us about the density fluctuation power spectrum (§6.2). We can also determine the abundances of clusters above T_X from X-ray satellite observations, above v_g from galaxy redshifts, or above v_{DM} from gravitational lensing. This should allow determination of not only the amplitude of the density fluctuations but also, over a limited band, the shapes (§6.3). Of course, *clusters aren't simple.*

Bulk flows have often been used to argue that large scale power exists over that in CDM models. We show what is required for CDM models to match these observations in §6.4. To construct galaxy flow maps, one needs redshifts to get the radial velocity and also estimates of distance, which are very hard to obtain in cosmology. The best data on galaxy flows uses the infrared Tully Fisher method, which combines 21 cm linewidths of spiral galaxies with their infrared flux observations, and relies upon a phenomenological relation between the velocity width and luminosity to estimate distance. Since we do not understand physically why this relation is as statistically tight as it appears to be, one should be cautious about overinterpreting the bulk flow data. It is after all the same Tully Fisher method that gives high $H_0 \sim 84$.

6.1 Galaxies and Large Scale Power

In Figure 3, the data for the angular correlation function derived from the APM survey is compared with theoretical predictions for the models of Table 1. The data shown include a downward offset of 0.002 suggested by Efstathiou [26] as the maximum possible error level. The spread of points is considered to be a reasonable estimate of the errors. Galaxies in different magnitude bins were scaled back from the $\sim 500\,h^{-1}$Mpc depth that the APM survey is sensitive to a depth of $\sim 300\,h^{-1}$Mpc, the depth of the Lick survey that Peebles used in constructing his famous 1,000,000 galaxy map; the APM team has found over 4×10^6 galaxies (down to magnitude 20.5) in their southern sky survey area, and use a subregion with 2×10^6 galaxies for their w_{gg} estimation. It is because of the sheer number of galaxies that one can do better statistically than the multi-thousand redshift surveys in spite of the information loss from radial projection.

There is an overall galaxy biasing scale that allows the curves to translate up or down, $b_g\sigma_8$. The naive biasing approach takes $b_g = \sigma_8^{-1}$ to give unity fluctuations in the galaxy number on $8\,h^{-1}$Mpc scales. This assumes that linear theory is valid, and it is amazing that it works so well. However, no nonlinear corrections were applied to the theoretical power spectra for the curves of Figure 3. For angular scales above $\sim 1°$ at the (scaled) depth of the catalogue

Figure 3: *The models of Table 1 are compared with the angular correlation function $w_{gg}(\theta)$ (dots) determined from the APM Galaxy Survey [19] (scaled to the depth of the Lick catalogue). No nonlinear corrections were applied to the theoretical power spectra, but for angular scales above $\sim 1°$ and for amplitude factors $\sigma_8 \lesssim 1$, the linear approximation is accurate. All but the standard CDM model agree reasonably well with the data.*

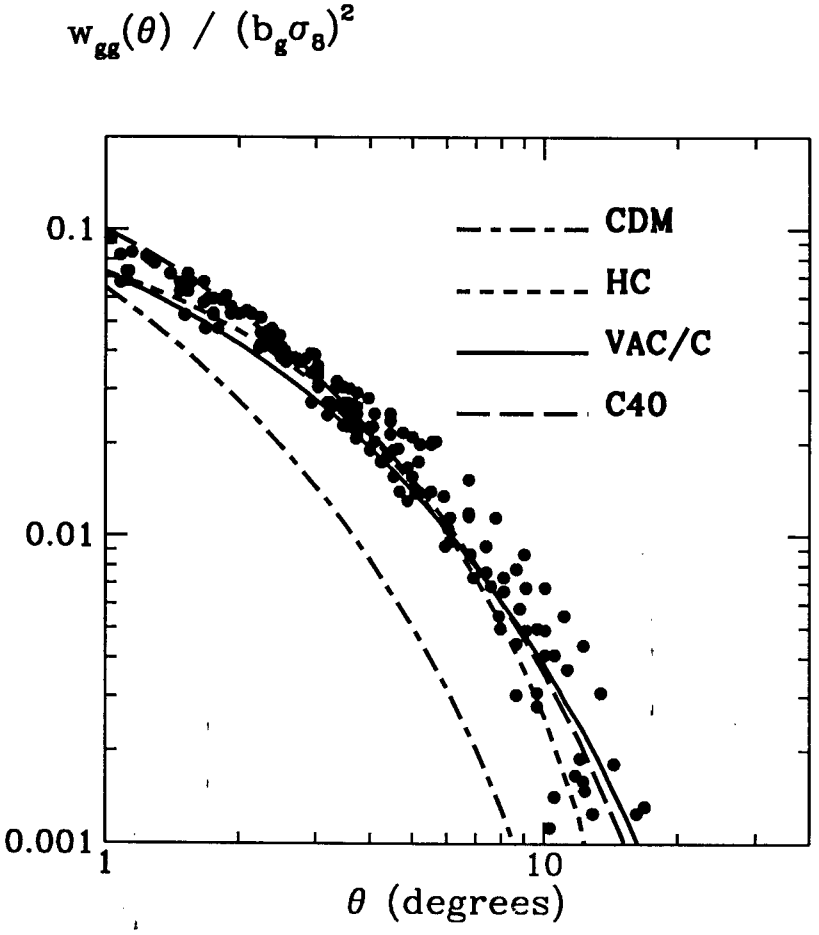

(corresponding to a physical scale of $\sim 5h^{-1}$Mpc), this should be accurate — although once amplitude factors σ_8 exceed unity there are modifications that help with the shape of the CDM model. Nonetheless b_g slightly in excess of σ_8^{-1} would help it, while for the C40 model b_g below σ_8^{-1} is probably needed so that w_{gg} agrees in the nonlinear regime below 1°.

The shape of the standard CDM model does not match the observations. Couchman and Carlberg [28] solved the dilemma for the CDM model by taking $\sigma_8 \approx 1.2$ and using nonlinear effects and a model for galaxy formation that gave less power on small scales than the mass distribution, *i.e.*, there was anti-biasing on small scales. Although there are other difficulties with such a high σ_8 amplitude, especially with the pair velocities of galaxies on small scales ($\sim 1\,h^{-1}$Mpc) and the abundances of high temperature clusters as a function of redshift (see Efstathiou, Bond and White [44] and §6.3), this does bring into focus that the formation of galaxies is such a complex gasdynamical event that linear scale-independent biasing, the key to relating galaxy observations to fundamental early universe physics, may in the future prove to have been remarkably naive.

6.2 Clusters and Large Scale Power

Clusters have been one of the main indicators of large scale power since the Bahcall and Soneira [45] and Klypin and Kopylov [46] 1983 estimations of the correlation length of Abell clusters. BBE [27] showed how dismally the CDM model fared with this data, but also that HC and VAC/C models fared much better (but still not enough for the vintage 1983 version of ξ_{cc}). Now the observations of ξ_{cc} appear to be compatible with the observations of w_{gg} [26]. Figure 4 shows that the ratio of ξ_{cc} to ξ_{gg} on large scales as predicted by the hierarchical peaks model of cluster formation described by Bond and Myers [47] for a w_{gg}–inspired power spectrum agrees with the data.

A shape compatibility between ξ_{cc} and ξ_{gg}, if it holds up, is very significant. Nonuniform biasing, $b_g(\vec{r},t)$, of galaxies relative to the mass distribution (due, *e.g.*, to gas dynamical, merging or radiative effects) could always be invoked to explain the excess power in ξ_{gg} relative to that in the $\xi_{\rho\rho}$ of the CDM model. However, the large biasing factor, b_c, of clusters is expected to be relatively uniform, since the thresholding criterion — '*have you collapsed by now?*' — is a local timing question. Thus biasing factors for galaxies may actually be relatively uniform too. Further, hierarchical peak theory predicts $[\xi_{cg}/\xi_{gg}]^{1/2} = (b_c/b_g)^{1/2}$ which Efstathiou [26] shows is a good approximation to his data. On the other hand, we must be wary of overinterpreting these new ξ_{cc}'s, since the samples are small and the error bars are large.

6.3 Clusters and σ_8

Cluster abundances provide an especially sensitive measure of σ_8, the conventional fluctuation normalizer. This is easy to see using a simple argument from Bardeen *et al.* [48] and Efstathiou, Bond and White [44]: an unperturbed sphere of radius $8\,h^{-1}$Mpc contains $1.2\times10^{15}\Omega_{nr}h_{50}^{-1}\,M_\odot$, and if the region when

Figure 4: *Cluster-cluster correlation amplitude as a function of cluster abundance for a power spectrum that reproduces the APM w_{gg} and ξ_{cc} data (solid curves, denoted by $\Gamma = 0.2$ as per ref. [44]), and also for the standard CDM model (short-dashed, $\Gamma = 0.5$). The upper curves (at small n_{cl}) for each of the two cases have $\sigma_8 = 1$, the lower have $\sigma_8 = 1.4$; biasing of clusters is so strong that their clustering is relatively insensitive to the amount of dynamics which σ_8 measures. A_1 and A_3 denote Abell richness 1 and 3 clusters (Bahcall and West [49], Postman et al. [50]), APM_0 and APM_1 refer to clusters found in the APM survey (Dalton et al. [24]) with an algorithm less subject to projection contamination than Abell's, and ED refers to the Edinburgh-Durham cluster sample found in the ROE Southern Sky catalogue (Nichol et al. [25]). CDM does not have enough LSS power to explain the shape of ξ_{cc}. To put ξ_{cc} relative to ξ_{gg}, a clustering length of $5.4\,h^{-1}$Mpc was adopted, as in Fig.1. The long-dashed curve is the Bahcall scaling law for the correlation strength with richness. Although it was motivated by a phenomenological fractal description, this figure shows it can be fully understood within Gaussian inflation fluctuation theory.*

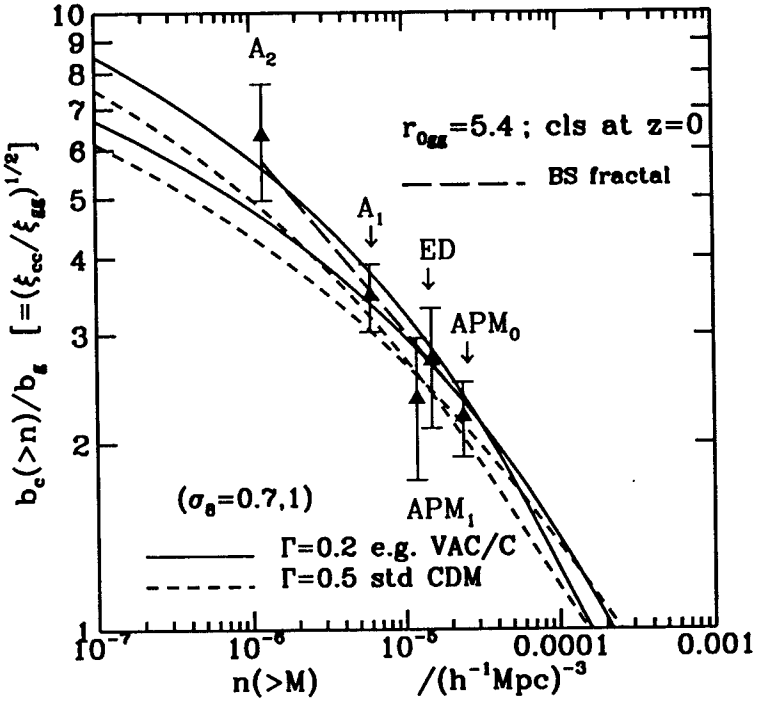

it virializes is compacted into an average overdensity of 178 relative to the background (as in spherical top hat collapses), then its final radius is nearly an Abell radius, $1.5\,h^{-1}$Mpc. If '3σ peaks' on this scale are virializing now, then $\sigma_8 \approx 0.6$ follows if we set $3\sigma_8 \approx 1.69$, where 1.69 is the average linear overdensity needed for a spherical shell to have collapsed to a point. If they virialized at $z = 0.2$, then $\sigma_8 \approx 0.7$.

BBE [27] give more precise estimates of the number of σ's required to get the Abell richness 1 abundance for clusters virializing now using the spherical approximation for the models in Table 1, among others. We got $\sigma_8 \approx 0.7$–0.8. Frenk *et al.* [51] got $\sigma_8 \approx 0.3$–0.5 based on projection corrections of cluster v_g's, Bond and Myers [47, 52] got $\sigma_8 \approx 0.6$–0.9 based on the Edge *et al.* [53] sample of X-ray clusters, and White *et al.* [54] got $\sigma_8 \approx 0.5$–0.6. Carlberg and Couchman [28] raised the spectre of σ_8 being in excess of unity, with the explanation of the paucity of very high velocity dispersion clusters a result of velocity biasing in which v_g/v_{DM} is substantially below unity; however, a large temperature biasing of X-ray clusters would also be required and this does not seem likely.

Quite small variations in σ_8 dramatically change the predicted number of high T_X and v_g clusters as a function of redshift. The data is still sufficiently murky that one can argue about a factor of two in σ_8, yet the situation is promising. To have at least one $T_X = 14$ keV cluster at redshift 0.2 — and one was found by the Ginga satellite (Arnaud *et al.* [55]) — strongly constrains how low σ_8 can be (provided complex gastrophysics does not modify the fully virialized assumption). Adams *et al.* [9] get $\sigma_8 > 0.7$. However, the richest cluster in Abell's catalogue, Abell 665 at $z = 0.18$, has a more modest $T_X = 8.2$ keV, so it is unclear how anomalous the Ginga cluster will turn out to be. (The Abell 665 Sunyaev-Zeldovich decrement is now well-observed, giving a $\Delta T/T = -1.46 \times 10^{-4}$ between cluster centre and cluster outskirts (Birkinshaw *et al.* [7]), which also agrees reasonably well with estimates obtained from the X-ray observations of bremsstrahlung from the hot cluster gas.)

The cluster system could also give the shape of σ_R around $R = 8\,h^{-1}$Mpc. Indeed, naive modelling of the current X-ray observations supports a shallower power spectrum than CDM gives over the spatial waveband responsible for cluster production, not unlike the one the w_{gg} data suggests, but this is even more dependent upon uncertain gasdynamical issues (Bond and Myers [47,52] and references therein).

Fortunately we are now in the midst of a world-wide assault on clusters, with the development of catalogues beyond Abell, using for example, the APM and ROE Southern Sky surveys (Dalton *et al.* [24], Nichol *et al.* [25]), with new X-ray satellites (ROSAT of course and BBXRT and the soon-to-be launched ASTRO-D which is in many ways ideal for cluster T_X determination), and multi-object spectrographs that can be used to get much more accurate v_g determinations. Sunyaev-Zeldovich experiments are also maturing, both in the radio, using the Owens Valley dishes (with COMA now seen in SZ), the 5 km array in Cambridge, and in the mm and sub-mm, aboard balloons. Accompanying this is a tremendous burst of theoretical work modelling with gas dynamics the realistic formation and evolution of clusters. Although theorists have a long way to go and much parameter space to cover, we can look forward to well-calibrated cluster models to wake theorists from their dreams: in a hierarchy, clusters will often have had a recent major merger, or be in the throes of one, equilibrium may well not prevail, and the core physics that X-rays probe is complicated by gas inhomogeneities, cooling flows, metals, magnetic fields, radio galaxies, *etc.*

6.4 Large-scale Streaming Velocities and σ_8

Large scale streaming velocities of galaxies directly probe the amplitude of the mass density fluctuations on large scales. This indicates a high amplitude for the spectrum (Bertschinger *et al.* [56], Efstathiou, Bond and White [44], Adams *et al.* [9]). From optical surveys, Bertschinger *et al.* estimated the three-dimensional velocity dispersions of galaxies within spheres of radius $40\,h^{-1}$Mpc and $60\,h^{-1}$Mpc (after the data had been smoothed with a Gaussian filter of $12\,h^{-1}$Mpc),

$$\sigma_v(40) = 388\,[1 \pm 0.17]\,, \sigma_v(60) = 327\,[1 \pm 0.25]\ (\mathrm{km\ s^{-1}})\,.$$

We have data for only the patch around us, so the theoretical spread expected is quite large. As a function of spectral index n_s, standard CDM models give

$$\sigma_v(40) = 300\,\sigma_8\,e^{1.06(1-n_s)}\,[1^{+.35}_{-.57}]\,, \sigma_v(60) = 238\,\sigma_8\,e^{1.19(1-n_s)}\,[1^{+.35}_{-.57}]\ (\mathrm{km\ s^{-1}})\,.$$

The range, $\sigma_8 \approx 1.29 e^{-1.06(1-n_s)}\,[1^{+.38}_{-.65}]$, suggested by the velocity data is similar to that obtained from DMR, but I should caution that these bulk flow estimates are not on as firm a foundation as the DMR measurement. For models with more LSS, lower values of σ_8 can explain the LSSV data. The velocities in the VAC/C model still require σ_8 in excess of unity, while C40 requires $\sigma_8 \sim 0.8$; but the errors are large.

7. The Gastrophysical Realms

Gastrophysics is important below about $8\,h^{-1}$Mpc, a band which forms clusters and also large voids. In Table 1, the redshifts z_{nl} signal when pervasive structure forms on those mass scales. For viable post-COBE models, there is a very large range: in some, galaxy halos would virialize at high redshift, and in others quite late. And even with specification of the halo formation epoch, dissipative phenomena greatly impede the translation into a full theory of galaxy formation.

The Hierarchy with Gastrophysical Processes: If our interests are just to nail down the parameters characterizing the primordial fluctuations, it is best to use clean probes, those on large scales where we do not expect gas dynamics to have had a large effect. This includes CMB anisotropies, and, we hope, large

scale streaming velocities. If biasing on large scales is a linear phenomenon, then the correlation functions of galaxies and clusters for $r \gtrsim 10\,h^{-1}$Mpc should be linear probes of the mass density fluctuations. However, such probes might be affected by gas dynamics (*e.g.*, environmental influences on the Tully-Fisher relation between infrared flux and 21 cm line widths of spiral galaxies could give false impressions of LSS flows [56]).

Merging: The essence of the hierarchy is merging and this may be the defining principle for the formation of the most interesting objects in the universe, the great energy releasers like starbursts and active galactic nuclei (AGNs) and radio galaxies. That close encounters will be important for them is suggested by their enhanced clustering over that of normal galaxies. And even the large scale galaxy distribution may depend upon the details of how galaxies merge in groups, since larger groups are more clustered than smaller groups and than general galaxies. (This was used in the Couchman and Carlberg [28] attempt to resurrect the CDM model.) In purely collisionless computations, galactic mass dark matter halos lose their identity to larger mass halos as the hierarchy develops. A challenge to gastrophysicists is to show the extent to which dissipation arrests this overmerging problem for galaxies themselves. Barnes and Hernquist [57] describe the current state-of-the-art on gaseous mergers.

Polluting Winds: The internal energy generation of big galaxies, especially of radio and active galaxies and starbursts, can have potentially devastating effects upon themselves and their environment. While the 10^{61} ergs released in these relatively rare seed structures could not trigger a chain reaction explosion scenario which generates all of the observed large scale structure as in the Cowie-Ostriker-Ikeuchi story, because of FIRAS constraints, they can stimulate star formation over moderate Mpc scales, and high redshift radio galaxy observations in fact show that this happens. We know slightly less energetic galactic superwinds exist in nearby galaxies (*e.g.*, M82, whose wind is known to spew forth kinetic energy, photons above the Lyman edge, dust and metals in gas form, magnetic fields, *etc.*). Arp 220 is the canonical starburst galaxy, with a far infrared flux of $\sim 10^{45}\,L_\odot$, a similar kinetic energy release in superwinds, yielding a total energy release of $\sim 10^{60}$ ergs with $\sim 10^9\,M_\odot$ consumed if the starburst has a duration of about $10^7 - 10^8$ years. Arp 220 is undoubtedly a merger, probably of two spirals, a phenomenon which should be ubiquitous in hierarchical models — especially at higher redshift when the merger rate is expected to have been higher. After all that is how giant galaxies would have been assembled in the hierarchy.

Feedback: Energy output from collapsed objects could enhance *or* damp structure development. Hierarchical models like the CDM model rely on feedback to suppress catastrophic star formation at $z \sim 10 - 20$, when gas clouds of about $10^6 - 10^7\,M_\odot$ collapse. Such small clouds are quite fragile, easily unbound by the energy they produce or by energy incident from outside. Later, at least by $z \sim 5$, we rely on feedback to highly ionize the intergalactic medium via UV photons or shock-heating to explain the Gunn-Peterson effect. The UV output from quasars and other AGNs come very close to explaining this, according to Meiksin and Madau [58]. A hot medium can significantly smooth the gas (over a scale $k^{-1} \sim 0.1\,h^{-1}$Mpc, *i.e.*, $\sim 10^{10}\,M_\odot$, if the temperature is 2×10^4K at $z = 5$), but not the dark matter, which clusters into deeper and deeper potential wells with larger and larger virial velocity dispersions until finally gas can begin to fall back in. Changing UV backgrounds could accentuate this late infall. Effects like these may have something to do with the mystery of faint blue galaxies.

Lyman Alpha Clouds and dGs: Tiny and moderate mass dwarfs are unfortunately more prone to feedback effects than larger galaxies are, because their potential wells are less deep. For example, a reasonable model of intergalactic gas clouds seen as the 'forest' of redshifted Lyman alpha absorption lines in the spectrum of quasars is that they are dwarf galaxies blowing apart. The properties of the Lyman α cloud system will probably depend crucially upon the amplitude $\sigma_{0.1}$, since if it is too high, as in the COBE-normalized CDM model, then dwarf galaxy scale objects would have virialized at high redshift and then merged into more massive entities, leaving Lyman α clouds to form in other ways, maybe as remnants of fragmenting shells from galactic winds. An even bigger puzzle in *all* models are the faint blue galaxies, a population which dramatically fades from view below $z \sim 0.3$ — a redshift of no obvious significance in the hierarchy.

Elliptical Ages and the Earliest QSOs: But we should contrast the dwarf galaxy puzzles that suggest lower values for $\sigma_{0.1}$ with the apparent venerable age of elliptical galaxies and globular clusters, and the existence of quasars at $z > 4$, which all point to significant early activity and thus high $\sigma_{0.5}$. Best estimates matching theoretical with observed galaxy spectra give elliptical galaxy formation at uncomfortably high redshifts between 10 and 20. This is anathema to all of the Table 1 models, even for the low bias factor models that the COBE result would indicate for the CDM model. And when quasars form may depend upon forming deep (albeit small mass) potential wells and therefore be sensitive to $\sigma_{0.1}$.

Cooling and Fragmentation: These processes are at least as fundamental to galaxy formation as feedback. After all one needs to transform the gas into stars, and it is difficult to be definitive about star formation in the Milky Way, let alone in unobserved high redshift environments. We expect that cooling and fragmentation will lead to a two-phase hot/cold (10^6K/10^4K) protogalactic medium, something that will be hard to include explicitly in full galaxy formation calculations because of the small size of the cool clouds.

FIRAS Constraints: Why have we not directly detected the waste heat of gastrophysical feedback? COBE's FIRAS experiment now limits the excess energy

from 500μ to 5000μ (the CMB peak is at 1400 μ) to be $\lesssim 3 \times 10^{-4}$ of the total in the CMB, as long as it deviates from a blackbody and does not mimic the Galactic spectrum fit to the FIRAS data (Mather *et al.* [1]). Even if some extragalactic component mimicked Galactic dust emission within the errors, there will still be a strong limit on high redshift luminous dust-shrouded starbursts, indeed so strong that energy we believe to be there would have to come out in another wavelength band. One could suppose the emitting dust is quite hot so the redshifted output would just avoid the FIRAS wavelengths; or assume starbursting at high redshift occurs in a dust-free environment (unlikely) so that the radiation comes out in the near infrared. The IR limits from COBE's DIRBE experiment are not yet that strong, being plagued by difficult foreground subtractions before the residual cosmological signal can be unearthed.

A Hydro Future: Detailed 3D gas dynamical codes for simulating the formation of cosmic structures are under active development. Unlike purely gravitational N-body studies, however, where the large distance structure is largely unaffected by the nonlinear evolution on small scales, gas processes are expected to couple small scales to larger ones. What this means computationally is that, given the finite resolutions that we are capable of following with 3D codes, we must model by hand what may be termed *sub-grid physics* to feed into an upward cascade of influence. Thus, star formation, supernova explosions, galactic winds, HII regions, ionized IGM, cooling instabilities and flows, fragmentation, dynamo generation of magnetic fields in collapsing objects, all of the problems that make interstellar medium studies so challenging, face us in cosmology now that we have entered the realms of gastrophysics.

The complexity of the physics operating at the (astrophysical) short-distance end of the spectrum reminds one of weather simulations, but cosmic weather we must do if we are to determine the fluctuation amplitudes in the USSS, VSSS, SSS and MSS wavebands rather than through theoretical extrapolations from larger scales. Fortunately the VLSS is unscathed by gastrophysical processing, and we have growing evidence that the LSS band is relatively untouched, so a detailed determination of the fluctuation spectrum on these scales is a physics problem for our time. After using multiresolution microwave background experiments to determine the cosmic parameters defining the unperturbed background, we can correct the spectrum for linear evolution. This primordial (post-inflation) spectrum would offer a glimpse of the fluctuation-generation physics that operated when our Hubble patch was very very young, and open a window to ultra-ultra high energies, far beyond what your accelerators can ever achieve. I shall end on this highly optimistic note.

Acknowledgements: In this review of the current state of our cosmological art, referencing is regrettably sporadic to the many who have made important contributions. Collaborative work with George Efstathiou, with Ed Cheng, Steve Meyer and Lyman Page, with Todd Gaier, Phil Lubin and Jeff Schuster, and with Steve Myers led to Figs. 2 and 3. This lecture overlaps considerably with a cosmological overview given by me at the Third Teton Summer School [59].

Appendix: Cosmology Primer for Particle Physicists

In this Appendix, we first review standard cosmological units and notation, then define the fluctuation power spectra which play such a large part in this paper. Length, mass and luminosity are usually expressed in terms of the megaparsec, Mpc $= 3.086 \times 10^{24}$ cm $= 3.26 \times 10^6$ light-years, the solar mass, $M_\odot = 2 \times 10^{33}$ grams, and the solar luminosity, $L_\odot = 3.86 \times 10^{33}$ erg/s. Since cosmological distances are usually estimated from redshifts by applying Hubble's law, a more appropriate cosmological unit of length is the h^{-1}Mpc, which is another name for 100 km s^{-1}. We use the h^{-1}Mpc often, even in theoretical models in which h is known.

The average mass density $\bar{\rho}_j$ for matter of type j is usually expressed in units of the critical density ρ_{cr} marking the boundary between open and closed universes: $\Omega_j \equiv \rho_j/\rho_{cr}$. The critical mass density is

$$\rho_{cr} = 1.12 \times 10^{-5}\, h^2\ m_N\, \mathrm{cm}^{-3} = 10.5\, h^2\ \mathrm{kev\,cm}^{-3} = 2.76 \times 10^{11}\, h^2\, M_\odot\ \mathrm{Mpc}^{-3}, \quad (A.1)$$

where m_N is the nucleon mass. More generally, we define at redshift z the density parameter $\Omega_j(z) \equiv \bar{\rho}_j(z)a^3/\rho_{cr}$. The expansion factor of the Universe a is taken to be unity now, so that it is related to the redshift z by $a \equiv (1+z)^{-1}$. Nonrelativistic matter has $\Omega_{nr}(z) = \Omega_{nr,0}$ independent of redshift, while relativistic matter has $\Omega_{er}(z) = \Omega_{er,0}a^{-1}$, decreasing in relative importance as the Universe expands. Vacuum energy (also associated with a nonzero cosmological constant Λ) has $\Omega_{vac}(z) = \Omega_{vac,0}\, a^3$, where $\Omega_{vac,0} = H_0^{-2}\Lambda/3$. We can also identify a curvature energy $\Omega_{curv} = [1-\Omega_{tot,0}]a$, where $\Omega_{tot,0} = \Omega_{er,0}+\Omega_{nr,0}+\Omega_{vac,0}$. Both Ω_{vac} and Ω_{curv} become progressively more important as the universe expands. The Friedmann equation for the expansion rate H expresses the vanishing of the super-Hamiltonian for FRW spaces, the energy constraint equation as derived from the ADM formulation of general relativity:

$$\left[\frac{1}{a}\frac{da}{dt}\right]^2 \equiv H^2 = \frac{8}{3}\pi G\left[\Omega_{er,0}a^{-4} + \Omega_{nr,0}a^{-3} + \Omega_{vac,0}a^0 + \Omega_{curv,0}a^{-2}\right]. \quad (A.2)$$

Light massive neutrinos have a more complicated form for $\Omega_{m\nu}(z)$, as do decaying particles. The photon density now is $\Omega_{\gamma,0} = 2.5 \times 10^{-5}h^{-2}$, and the total density in relativistic particles is $\Omega_{er,0} = 4.2 \times 10^{-5}h^{-2}$, including photons and three massless neutrino flavours. (In the standard Hot Big Bang Model, the current neutrino temperature is related to the observed photon temperature $T_{\gamma,0} \approx 2.73$K by $T_{\nu,0} = (4/11)^{1/3}T_{\gamma,0} \approx 1.96$K.) Dynamical constraints give $-1 \lesssim \Omega_{curv,0} \lesssim 0.8$, $\Omega_{vac,0} \lesssim 0.8$, and, for the density of matter which can cluster, $\Omega_{nr} \gtrsim 0.2$. Ω_{nr} is also compatible with unity. One component of nonrelativistic matter is of course baryons. Standard primordial nucleosynthesis strongly constrains the value of Ω_B (§2). Of course $\Omega_{curv} < 0$ is required for closure of the universe, and $|\Omega_{curv}| \lesssim 10^{-5}$ is the main (unavoidable) prediction

of inflation, with no strong sentiment on whether our local patch of the Universe should have Ω_{curv} positive or negative.

The dark matter which accounts for at least 90% of the mass density of the Universe may consist of a baryonic component, but if we want to have $\Omega_{curv} \approx 0$ and believe in the primordial nucleosynthesis constraint on Ω_B, we must assume the DM is primarily in non-baryonic form, such as massive elementary particle relics of the Big Bang. We classify the relic DM according to the magnitude of their primordial random velocities: hot DM, warm DM and cold DM. Particles which decoupled when they were relativistic ($m_\nu \ll T_{dec}$) at a temperature T_{dec} below that of the quark–hadron phase transition, ~ 200 MeV $= 2 \times 10^{12}$K, are called hot dark matter. The prototype is the light massive neutrino with mass of order 30 eV. Massive particles which decoupled when nonrelativistic are cold dark matter (CDM) candidates. They have negligible random velocities. CDM with weak interactions are often called WIMPs. An intermediate possibility between hot and cold is warm DM: particles which decoupled when relativistic, but at a temperature above the quark–hadron phase transition; a higher T_{dec} results in a lower velocity dispersion than in the hot DM case. It is also possible that at least some of the DM particles could decay, and some could be relativistic decay products. Vacuum energy does not cluster at all and could account for most of the dark matter.

Certain redshifts play particularly important roles in cosmology:

$$z_{eq} \equiv \Omega_{nr,0}/\Omega_{er,0} - 1 \approx 25000 h^{-2},$$

the epoch when the Universe passes from domination by relativistic particles to domination by non-relativistic ones; $z_{curv} = \Omega_{nr}^{-1}$, when the Universe passes from non-relativistic matter domination to curvature domination; $z_{vac} \approx [\Omega_{vac}/\Omega_{nr}]^{1/3} - 1$ when it passes to vacuum domination; z_{dec}, the redshift of photon decoupling, ≈ 1000 for normal recombination of the hydrogen plasma, and ~ 200 if the Universe remains ionized. The redshift of galaxy formation is unknown, but is probably between 3 and 10. The redshift when the first objects collapse is even less well known: it could be as high as $z \sim 1000$ or as low as $z \sim 4.7$, the redshift of the most distant observed quasar.

One of the major reasons for introducing inflation is to solve the horizon problem. The characteristic comoving scale over which information can propagate during an expansion time is the comoving Hubble length. Provided the redshift is large compared with z_{curv} and z_{vac}, we have

$$(Ha)^{-1} = H_0^{-1} \Omega_{er,0}^{-1/2} \left(\frac{T_\nu}{0.169\,\mathrm{MeV}}\right)^{-1} \left(\frac{g_e(T_\nu)}{10.75}\right)^{-1/6} \left[1 + \frac{\Omega_{nr,0}}{\Omega_{er,0}} \left(\frac{T_\nu}{0.169\,\mathrm{MeV}}\right)^{-1}\right]^{-1/2} . \qquad (A.3a)$$

At high redshift in the radiation-dominated regime, this is

$$(Ha)^{-1} \approx 77 \left(\frac{T_\nu}{1\,\mathrm{MeV}}\right)^{-1} \left(\frac{g_e(T_\nu)}{10.75}\right)^{-1/6} \text{ parsecs}, \quad z \gg z_{eq} . \qquad (A.3b)$$

In the matter-dominated regime

$$(Ha)^{-1} \approx 3000\, \Omega_{nr}^{-1/2} (1+z)^{-1/2}\, h^{-1}\mathrm{Mpc}, \quad z_{eq} \gg z \gg \Omega_{nr}^{-1} . \qquad (A.3c)$$

The effective number of relativistic degrees-of-freedom just prior to neutrino decoupling at $T_\nu \sim 1$ MeV is $g_e \approx 10.75$. At the quark-hadron phase transition, $g_e \sim 60$ and at Grand Unified energies it is a few hundred. We have used the approximate temperature-redshift relation

$$T_\nu \approx 1.69 \times 10^{-4} \left(\frac{g_e(T_\nu)}{10.75}\right)^{-1/3} (1+z)\ \mathrm{eV}, \qquad (A.4)$$

derived from conservation of the entropy per comoving volume. With a normal radiation–dominated early universe, the comoving scale associated with a galaxy, ~ 1 Mpc, is larger than the comoving Hubble length until T_ν drops to ~ 100 eV, at $z \sim 10^6$, with the consequence that primordial perturbations of sufficient amplitude for galaxy formation are difficult to construct; by z_{dec} only regions within $\sim 100\, h^{-1}$Mpc would have communicated, making the global isotropy of the cosmic background radiation temperature and the apparent large scale homogeneity of radio galaxies difficult to understand.

With the early vacuum energy dominance posited for inflation, $(Ha)^{-1} \sim a^{-1}$ decreases from some initial value $(Ha)_{inf}^{-1}$ as expansion proceeds, so $(Ha)^{-1}$ sweeps in to encompass ever *smaller* comoving length scales, arresting causal communication across waves with $k^{-1} > (Ha)^{-1}$. Indeed the general definition of inflation, that there is accelerated expansion, $\ddot{a} > 0$, rather than the normal deceleration, is precisely the condition that $(Ha)^{-1}$ decreases with time; an equation of state with $p/\rho < -1/3$, where p is the total pressure and ρ is the total energy density, is required, a condition realizable for scalar fields whose energy density is potential–dominated. With inflation, the comoving scale over which there could have been causal contact by now is then the usual formula, eq. (A.3a), *plus* $(Ha)_{inf}^{-1}$, allowing causal processes to be invoked for homogeneity and isotropy, as well as for fluctuation generation, provided the inflating region expands to $\gg H_0^{-1}$ in size. This is realizable if the number of e-foldings of expansion during inflation is $\gtrsim 70$, augmenting the ~ 60 e-foldings of the radiation and matter dominated epochs.

The slowing of the evolution rate that occurs around z_{eq} implies density fluctuations can grow more easily by gravitational instability, hence the horizon scale at that time is particularly significant for large scale structure: $(Ha)_{eq}^{-1} \approx 19 \Omega_{nr,0}^{-1/2}\, h^{-1}$Mpc. For example, it is the only scale required to specify the adiabatic scale–invariant cold dark matter model, the minimal inflation model used as the standard by which other models were generally judged over the past decade.

Even before the advent of inflation models of fluctuation generation, it was most often assumed that the linear perturbations formed a homogeneous and

isotropic Gaussian random field. In this case, a single function $\mathcal{P}_\rho(k)$ fully specifies the nature of the perturbation field. The density fluctuation spectrum,

$$\mathcal{P}_\rho(k) \equiv \frac{d\sigma_\rho^2}{d\ln k} \equiv \frac{k^3}{2\pi^2}\langle|(\delta\rho/\rho)(k)|^2\rangle, \qquad (A.5)$$

gives the contribution of (statistically independent) modes of comoving wavenumber $\vec{k}$ to the *rms* linear density fluctuations σ_ρ. Most inflation models do predict Gaussian perturbations, but there are theories of fluctuation generation with reasonable particle physics motivation that give non-Gaussian perturbations (see §3).

A major goal of cosmic structure research is to therefore ascertain whether the perturbations were initially Gaussian–distributed, and, if so, to determine the two-point function $d\sigma_\rho^2/d\ln k$. Although the form of the statistics is maintained in the linear regime, as the Universe evolves into the nonlinear regime the coupling of modes causes high order correlations to develop, obscuring the simplicity of the initial state of the perturbations. Linearity *is* an appropriate approximation for anisotropies in the cosmic microwave background radiation and for some aspects of large scale galaxy flows and clustering. Because these offer cleaner tests of the primordial fluctuation spectrum, they are given special attention in this paper.

Within linear perturbation theory, fluctuations can be decomposed into scalar, vector (vorticity) and tensor (gravitational wave) modes. Only the scalar modes are likely to be significant for structure formation. There are two main modes for scalar perturbations: adiabatic fluctuations — with perturbations in the total energy density and hence in the curvature — and isocurvature fluctuations — with perturbations in the energy densities of the various species of matter present, but not in the total. In inflation, adiabatic fluctuations arise from quantum zero point oscillations in the deSitter vacuum of the inflaton scalar field whose potential energy drives inflation. With only one scalar field of dynamical importance, approximate scale invariance for the spectrum of scalar field (ϕ) fluctuations $\mathcal{P}_\phi(k)$ is the natural outcome: once the wavelength exceeds the Hubble length, $\mathcal{P}_\phi^{1/2}(k)$ is approximately equal to the Hawking temperature $H(\phi)/(2\pi)$; provided the Hubble parameter is slowly varying, $\mathcal{P}_\phi^{1/2}(k)$ is nearly constant. For adiabatic perturbations, the post–inflation geometry, as described by a relativistic extension of the Newtonian gravitational potential, Φ, is also scale invariant: $\mathcal{P}_\Phi(k) \propto \mathcal{P}_\phi \approx$ constant. (The Poisson-Newton equation $a^{-2}\nabla^2\Phi = 4\pi G\delta\rho$ for the gravitational potential in an infinite expanding background remains an exact relation in general relativistic perturbation theory if $\delta\rho$ is the density perturbation in the comoving frame, and $-\Phi$ is a gauge invariant variable introduced by Bardeen [60]. Consequently the post–inflation density spectrum is $\mathcal{P}_\rho(k) \propto k^4$, which is called the Harrison–Zeldovich spectrum.)

The isocurvature mode might also be generated in inflation models, with fluctuations in some matter density component (baryons or cold dark matter) compensated by fluctuations of opposite sign in the radiation (photons, quark-antiquark pairs, gluons, etc.) at the epoch of generation. For isocurvature CDM perturbations, zero point oscillations in a pseudo-Goldstone boson field $\mathcal{A}$ such as the axion translate into nonrelativistic mass density perturbations upon mass generation: $\mathcal{P}_{\rho_\mathcal{A}}(k) \propto \mathcal{P}_\mathcal{A}(k)$. For isocurvature baryon perturbations (once referred to as isothermal or entropy perturbations), $\mathcal{P}_{n_B}(k)$ would be proportional to the oscillations in some field to which the baryon number density n_B couples. Thus, scale invariance of the scalar field implies scale invariance of the axion or baryon density perturbations, whereas $\mathcal{P}_\Phi$ vanishes at the time when either the axion mass or the baryon number is generated. It takes an artfully constructed fluctuation-generation model to get isocurvature perturbations that could be useful for cosmic structure formation (§3).

References

[1] Mather, J.C. *et al.*: 1993, *COBE preprint*.
[2] Olive, K.A., Schramm, D.N., Steigman, G., & Walker, T.P.: 1990, *Phys. Lett. B* **236**, 454; Steigman, G. *et al.*: 1992, preprint.
[3] Renzini, A.: 1992, *Proc. Texas/PASCOS Conference*.
[4] Tonry, J.: 1992, *Proc. Texas/PASCOS Conference*.
[5] Sandage, A. *et al.*: 1992, *preprint*.
[6] Kirshner, R. *et al.*: 1992, *Harvard preprint*.
[7] Birkinshaw, M., Hughes, J.P., & Arnaud, K.A.: 1991, *Astrophys. J.* **379**, 466.
[8] Freese, K., Frieman, J.A.,& Olinto, A.V.: 1990, *Phys. Rev. Lett.* **65**, 3233.
[9] Adams, F.C., Bond, J.R., Freese, K., Frieman, J.A. and Olinto, A.V.: 1993, *Phys. Rev.* **D 47**, 426.
[10] Salopek, D.S., Bond, J.R.,& Bardeen, J.M.: 1989, *Phys. Rev. D.* **40**, 1753.
[11] Bond, J.R. & Efstathiou, G.: 1987, *Mon. Not. R. astr. Soc.* **226**, 665.
[12] Smoot, G.F. *et al.*: 1992, *Astrophys. J. Lett.* **396**, L1.
[13] Wright, E.L. *et al.*: 1992, *Astrophys. J. Lett.* **396**, L13.
[14] Page, L.A., Cheng, E.S., & Meyer, S.S.: 1990, *Astrophys. J. Lett.* **355**, L1.
[15] Gaier, T., Schuster, J., Gunderson, J., Koch, T., Seiffert, M., Meinhold, P., & Lubin, P.: 1992, *Astrophys. J. Lett.* **398**, L1.
[16] Schuster, J. *et al.*: 1993, *UCSB preprint*.
[17] Meinhold, P.,& Lubin, P.: 1991, *Astrophys. J. Lett* **370**, 11.
[18] Readhead, A.C.S. *et al.*: 1989, *Astrophys. J.* **346**, 556.
[19] Maddox, S.J., Efstathiou, G., & Sutherland, W.J.: 1990, *Mon. Not. R. astr. Soc.* **246**, 433.
[20] Collins, C.A., Nichol, R.C.,& Lumsden, S.L.: 1992, *Mon. Not. R. astr. Soc.* **254**, 295.
[21] Kaiser, N., Efstathiou, G., Ellis, R.S., Frenk, C.S., Lawrence, A., Rowan-Robinson, M., & Saunders, W.: 1991, *Mon. Not. R. astr. Soc.* **252**, 1.
[22] Fisher, K.B., Davis, M., Strauss, M.A., Yahil, A., & Huchra, J.P.: 1992, *Astrophys. J.* , in press.
[23] Vogeley, M.S., Park, C., Geller, M.J.,& Huchra, J.P.: 1992, *Astrophys. J. Lett.* **391**, L5.
[24] Dalton, G.D., Efstathiou, G., Maddox, S.J., & Sutherland, W.J.: 1992, *Astrophys. J. Lett.* **390**, L1.
[25] Nichol, R.C., Collins, C.A., Guzzo, L.,& Lumsden, S.L.: 1992, *Mon. Not. R. astr. Soc.* **255**, 21p.
[26] Efstathiou, G.: 1992, *Proc. Nat. Acad. Sci.*, in press.
[27] Bardeen, J.M., Bond, J.R., & Efstathiou, G.: 1987, *Astrophys. J.* **321**, 18.
[28] Couchman, H.M.P. & Carlberg, R.G.: 1992, *Astrophys. J.* **389**, 453.
[29] van Dalen, A. & Schaeffer, R.K.: 1992, *preprint*.
[30] Davis, M., Summers, F.J., & Schlegel, D.: 1992, *Berkeley preprint*.
[31] Klypin, A.A. *et al.* : 1992, *preprint*.
[32] Bennett, D.P., Bouchet, F.R., & Stebbins, A.: 1992, *preprint*.
[33] Bennett, D.P. & Rhie, S.H.: 1992, *Livermore preprint*.
[34] Pen, U., Spergel, D.,& Turok, N.: 1993, *Princeton preprint*.
[35] Park, C., Spergel, D.,& Turok, N.: 1991, *Astrophys. J. Lett.* **372**, L53.
[36] Bond, J.R. & Efstathiou, G.: 1991, *Physics Letters B* **379**, 440.
[37] Seljak, U. & Bertschinger, E.: 1992, *MIT preprint*.
[38] Bennett, C. *et al.* : 1992, *Astrophys. J. Lett.* **396**, L7.
[39] Gould, A.: 1992, *IAS preprint*.
[40] Starobinsky, A.A.: 1985, *Soviet Astron. Lett* **11**, 133.
[41] Abbott, L. & Wise, M.: 1984, *Nucl. Phys.* **B244**, 541.
[42] Ganga, K. *et al.* : 1992, *Proc. Texas/PASCOS Conference*.
[43] Bond, J.R. & Efstathiou, G.: 1993, *preprint*.
[44] Efstathiou, G., Bond, J.R., & White, S.D.M.: 1992, *Mon. Not. R. astr. Soc.* **258**, 1P.
[45] Bahcall, N. & Soneira, R.: 1983, *Astrophys. J.* **270**, 70.
[46] Klypin, A.A. & Kopylov, A.I.: 1983, *Sov. Astron. Lett.* **9**, 41.
[47] Bond, J.R. & Myers, S.: 1991, *Trends in Astroparticle Physics*, ed. D. Cline & R. Peccei (Singapore: World Scientific), 262.
[48] Bardeen, J. M., Bond, J. R., Kaiser, N., & Szalay, A. S.: 1986, *Astrophys. J.* **304**, 15.
[49] Bahcall, N. & West, M.: 1992, *Ap. J.* **270**, 70.
[50] Postman, M., Geller, M., & Huchra, J.: 1992, *Astrophys. J.* **384**, 404.
[51] Frenk, C.S., White, S.D.M., Efstathiou, G. & Davis, M.: 1990, *Astrophys. J.* **351**, 10.
[52] Bond, J.R. & Myers, S.T.: 1992, *in Evolution of Galaxies and Their Environment* , Proceedings of the Third Teton Summer School, ed. M. Shull, & H. Thronson (Dordrecht: Kluwer).
[53] Edge, A.C., Stewart, G.C., Fabian, A.C., & Arnaud, K.A.: 1990, *Mon. Not. R. astr. Soc.* **245**, 559.
[54] White, S.D.M., Efstathiou, G.,& Frenk, C.S.: 1992, *preprint*.
[55] Arnaud, K. *et al.* : 1992, *preprint*.
[56] Bertschinger, E., Dekel, A., Faber, S.M., Dressler, A., & Burstein, D.: 1990, *Astrophys. J.* **364**, 370.
[57] Barnes, J. & Hernquist, L.: 1992, *Ann. Rev. Astron. Ap.* **30**, 705.
[58] Meiksin, A. & Madau, P.: 1993, *CITA preprint*.
[59] Bond, J.R.: 1992, *in Evolution of Galaxies and Their Environment* , Proceedings of the Third Teton Summer School, ed. M. Shull and H. Thronson (Dordrecht: Kluwer).
[60] Bardeen, J. M.: 1980, *Phys. Rev.* D22, 1882.